

MoEdit: On Learning Quantity Perception for Multi-object Image Editing

Yanfeng Li¹ Kahou Chan¹ Yue Sun¹ Chantong Lam¹ Tong Tong²

Zitong Yu³ Keren Fu⁴ Xiaohong Liu^{5*} Tao Tan^{1*}

¹ Macao Polytechnic University ² Fuzhou University ³ Great Bay University

⁴ Sichuan University ⁵ Shanghai Jiao Tong University

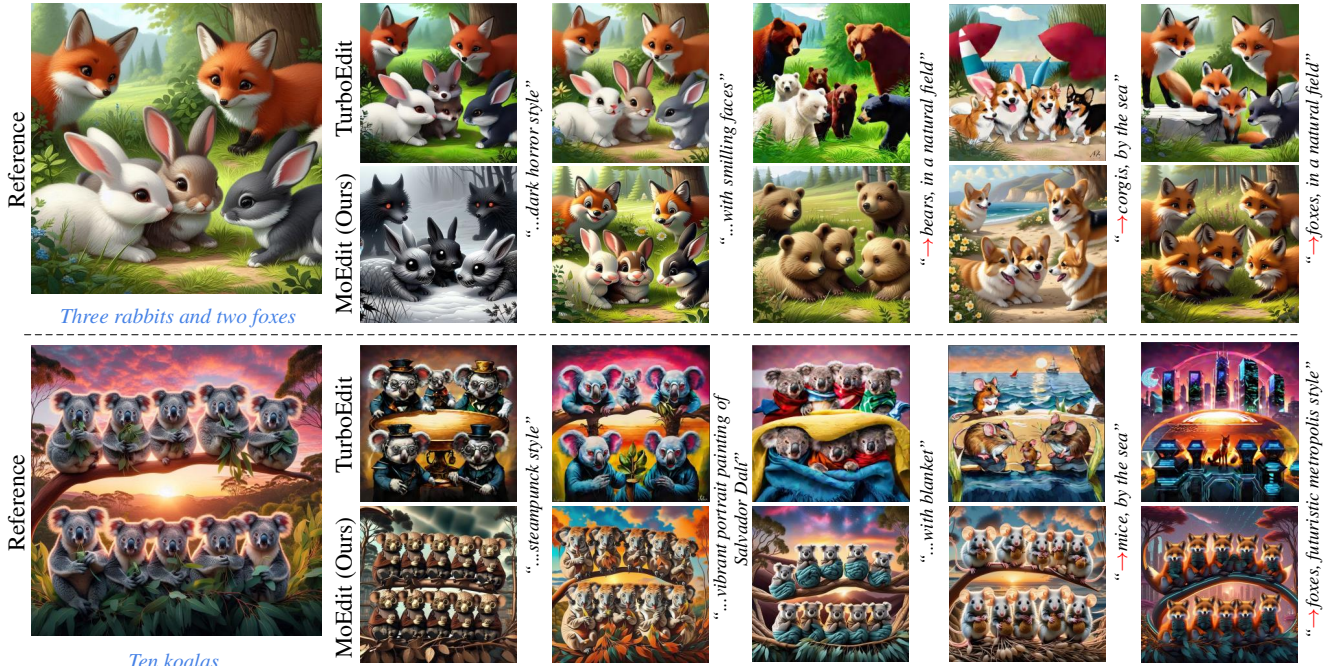


Figure 1. Visual comparisons of our MoEdit with TurboEdit [52]. Reference represents input images. Five different images edited by each method are based on five distinct text prompts.

Abstract

Multi-object images are prevalent in various real-world scenarios, including augmented reality, advertisement design, and medical imaging. Efficient and precise editing of these images is critical for these applications. With the advent of Stable Diffusion (SD), high-quality image generation and editing have entered a new era. However, existing methods often struggle to consider each object both individually and part of the whole image editing, both of which are crucial for ensuring consistent quantity perception, resulting in suboptimal perceptual performance. To address these challenges, we propose MoEdit, an auxiliary-free multi-object image editing framework. MoEdit facilitates high-quality multi-object image editing in terms of style trans-

fer, object reinvention, and background regeneration, while ensuring consistent quantity perception between inputs and outputs, even with a large number of objects. To achieve this, we introduce the Feature Compensation (FeCom) module, which ensures the distinction and separability of each object attribute by minimizing the in-between interlacing. Additionally, we present the Quantity Attention (QTTN) module, which perceives and preserves quantity consistency by effective control in editing, without relying on auxiliary tools. By leveraging the SD model, MoEdit enables customized preservation and modification of specific concepts in inputs with high quality. Experimental results demonstrate that our MoEdit achieves State-Of-The-Art (SOTA) performance in multi-object image editing. Data and codes will be available at <https://github.com/Tear-kitty/MoEdit>.

* Corresponding author.

1. Introduction

Multi-object image editing enables flexible modification of various concepts in images while maintaining overall visual coherence [3]. These techniques are essential for applications such as image generation [27, 36], medical imaging [37, 48], and augmented reality [2, 21, 26].

Despite its importance, editing multi-object images remains a challenging task due to existing methods struggling to consider each object both individually and part of the whole image. This often results in inconsistent quantity perception during editing, leading to visual distortions, blurring, and disruptions in scene semantics and logical structure, as well as reduced editability [24, 46].

Traditional techniques typically focus on enhancing single-object editing by fine-tuning methods such as Stable Diffusion (SD) locally, but fail to ensure consistent quantity perception across multiple objects [13, 30, 37]. Recent approaches leveraging Large Language Models (LLMs) for text-image alignment have focused on maintaining consistency in the global information of the whole image. While these methods ensure quantity consistency visually [51, 54], they often encounter aliasing of object attributes. This oversight makes the effective extraction of object attributes difficult during editing [29, 40]. Auxiliary tools, such as masks, are commonly used to extract object attributes [1, 5]. While effective, this approach fails to capture global image information of the whole image and requires a one-to-one association between auxiliary tools and each object to preserve quantity consistency. This significantly increases training costs, reduces user convenience, and often demands manual adjustments. Therefore, there is an urgent need for a solution that extracts object attributes from the whole image, ensuring the distinction and separability of these attributes while simultaneously perceiving global information of the whole image. Such a solution would eliminate the need for consistent auxiliary tool quantities and address limitations in the multi-object image editing.

To address this technical challenge, we propose the MoEdit pipeline, an auxiliary-free solution designed to enhance the editing quality and editability of multi-object images by ensuring consistent quantity perception between inputs and outputs. Our approach comprises two key modules: (1) Feature Compensation (FeCom) module: A feature attention is employed to enable interaction between text prompts, which contain quantity and object information, and the inferior image features extracted by the image encoder of CLIP [34]. This process compensates for inferior features to minimize the in-between interlacing, and ultimately extracts object attributes. The enhanced attribute distinction of each object also provides a foundation for the QTTN module to achieve auxiliary-free quantity perception. (2) Quantity Attention (QTTN) module: Without relying on any auxiliary tools, this module perceives

the information of each object both individually and part of the whole image from the image features enhanced by FeCom. The perceived information is then injected into specific blocks of U-Net [32], enabling the model to acquire a clear and consistent quantity perception. The visual comparisons of our MoEdit with the latest method TurboEdit [52] is shown in Fig. 1.

Our contributions are as follows:

- We propose a novel pipeline named MoEdit to pioneer consistent quantity perception for multi-object image editing, even with a large number of objects. This design provides inspiring insights for such challenges.
- We introduce the FeCom and QTTN modules to extract object attributes and preserve quantity consistency without auxiliary tools, respectively.
- Compared to existing methods, MoEdit shows the SOTA performance in the preservation of quantity consistency, visual quality and editability.

2. Related Works

2.1. Text-to-Image Diffusion Models

Diffusion models have emerged as a groundbreaking research direction. These models are widely utilized in video generation [18, 19, 25, 56], QR code generation [7, 49], and audio synthesis [4, 16, 55]. Among these applications, Text-to-Image diffusion (T2I) models, which generate images from user-provided textual prompts, have garnered significant attention [6, 22, 64]. Furthermore, the generated images also provide reliable data sources for advancing the field of image quality assessment [17, 61, 63].

2.2. Image Editing

The application of diffusion models to image editing can be categorized into three primary approaches: (1) fine-tuning approaches: Methods like Imagic [14] fine-tune diffusion models using the original image or target prompts [44, 60]. While effective for specific tasks, these methods face reduced efficiency. (2) internal representation approaches: This line of research leverages internal model representations to address efficiency bottlenecks without requiring fine-tuning [23, 41, 53]. However, these methods often struggle to maintain the original structure and details in certain tasks. (3) inversion optimization approaches: A third category focuses on enhancing inversion processes to minimize errors during generation [12, 42]. Techniques like WaveOpt-Estimator [15] and Null-text Inversion [29] improve detail preservation and structural stability while significantly enhancing editing efficiency. Despite their advantages, these methods only target single-object attribute.

2.3. Quantity Perception in Image Generation

Consistent quantity perception requires models to consider each object both individually and part of the whole image.

Method	w/o LLM	w/o Guidance	Base Model	Quantity Consistency	Object Attributes
SSR-Encoder [59]	✓	✗	SD1.5	✗	✓
λ -Eclipse [31]	✓	✓	Kandinsky	✗	✗
IP-Adapter [57]	✓	✓	SDXL	✗	✗
Blip-diffusion [20]	✗	✓	SD1.5	✗	✗
MS-diffusion [45]	✓	✓	SDXL	✗	✓
Emu2 [39]	✗	✓	SDXL	✓	✗
TurboEdit [52]	✗	✓	SDXL	✓	✗
MoEdit (ours)	✓	✓	SDXL	✓	✓

Table 1. An overview of previous studies. “w/o LLM” and “w/o Guidance” indicate whether the model utilizes an LLM or specific guidance as auxiliaries, respectively. Object Attributes and Quantity Consistency denote whether the method considers each object individually or part of the whole image, respectively.

This capability allows a model to understand the interplay between quantity, semantics, and image structure. Some approaches leverage LLMs to align textual and visual elements for finer editing [51]. However, they often neglect to ensure the distinction and separability of each object attribute [10, 20, 47]. Methods like SLD [62], TurboEdit [52], and Emu2 [39] achieve visual consistency in quantity but are constrained to editing a single object in multi-object scenarios, limiting their broader applicability. In contrast, object-centered approaches such as LoMOE [3], MS-diffusion [45], and SSR-Encoder [59] use masks, bounding boxes, or dedicated target queries to extract individual object attributes. While effective, these methods face challenges in modeling each object as part of the whole image, necessitating one-to-one associations with auxiliary tools to preserve quantity consistency. However, this reliance on auxiliary tools increases both training complexity and cost, reducing user convenience. In this work, we propose a pipeline that can effectively extract object attributes and preserve quantity consistency without auxiliaries (LLM and Guidance). It simply and efficiently implements quantity perception for multi-object images. Some previous methods are reported in Table 1.

3. Method

3.1. Overall

We propose MoEdit, denoted as \mathcal{G} , with its architecture illustrated in Fig. 2. MoEdit builds upon the foundation of the SD model, extending its capabilities to perceive the information of each object both individually and part of the whole image within input image I . This ensures a clear understanding of quantity perception while preserving attributes of each object.

The primary objective of MoEdit is to preserve quantity consistency in multi-object image editing, thereby delivering high-quality results that are more closely aligned with user expectations. The edited output image $I_e = \mathcal{G}(c_e, c_q, I, z_0)$ is generated based on two textual conditions c_e and c_q , an image condition I , and noise z_0 . Specifically,

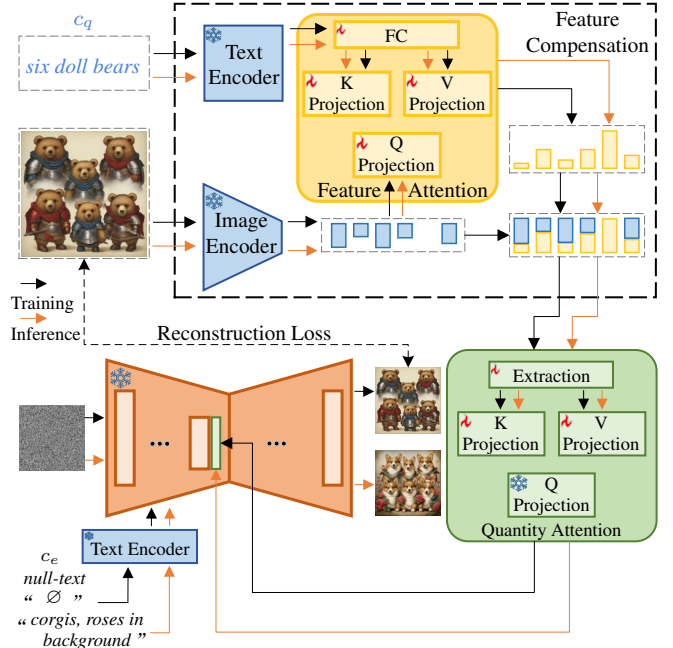


Figure 2. The framework of our propose method. The Feature Compensation (FeCom) module uses text prompts with quantity and object information to compensate for the inferior image features extracted by the image encoder of the CLIP. The compensated image features are then processed by the Quantity Attention (QTTN) module to conduct consistent quantity perception, which are injected into the U-Net to control image editing. During training, the text prompts is set to null-text. During inference, the text prompts can be modified to edit images.

c_e denotes the editing instruction, while c_q serves as a caption specifying the names and quantities of objects present in the input image. The architecture achieves these objectives through two modules: the FeCom and QTTN module.

The FeCom module, denoted as \mathcal{F} , processes the user-provided inputs I and c_q . This module bridges user-defined text prompts, which contain quantity and object information, with the inferior CLIP-encoded features extracted from the input image I , minimizing in-between interlacing to achieve the extraction of object attributes. The output of the FeCom module is a set of enhanced image features I_g , which ensure the distinction and separability of each object attribute, serving as input for the subsequent QTTN module.

The QTTN module, denoted as \mathcal{Q} , considers to perceive the information of each object both individually and part of the whole context within I_g . By injecting this information into a specific block of the U-Net, QTTN enables to preserve quantity consistency by effective control in editing process, without relying on auxiliary tools. This ensures efficient editing performance and high editability.

During the training phase, c_e is set as a null-text input to isolate the learning of consistent quantity perception from

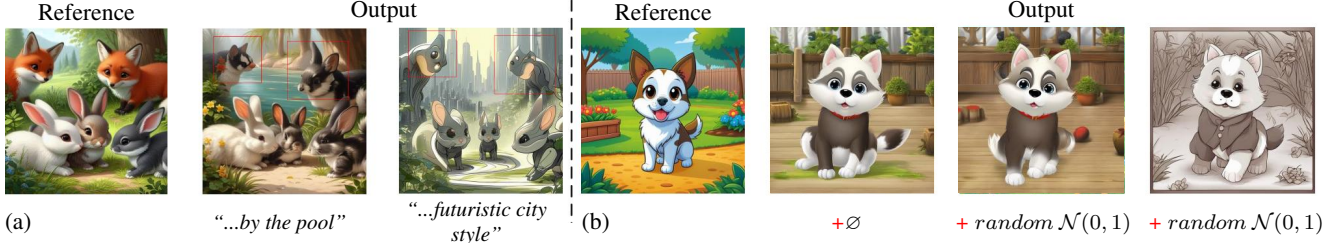


Figure 3. The illustration of the purpose of FeCom module. Reference denotes the input image. (a) When only the CLIP-encoded image information is used to represent I_g as input to the QTTN module, the attributes of foxes are either lost or shifted towards the attributes of rabbits, resulting in attributes aliasing. (b) The three images illustrate the results of adding three different Gaussian noises, $\mathcal{N}(0, 1)$, to $CLIP(I)$. This process alters the object attributes, background, and style while maintaining the structure and clarity of the image.

textual embedding interference. This design allows the FeCom and QTTN modules to focus on their respective tasks. At inference, c_e can be customized by users to guide the generation of high-quality images that meet their specific expectations. The subsequent sections detail the design and implementation of the FeCom and QTTN modules, along with the training and inference stages.

3.2. Feature Compensation

Relying solely on image features encoded by CLIP to represent I_g as input to the QTTN module often leads to aliasing of object attributes, as shown in Fig. 3 (a). This issue stems from strength of CLIP in capturing general visual semantics, yet its difficulty in encoding distinct, separable features in multi-object images. To mitigate this, the FeCom module leverages user-provided text prompts, which contain object and quantity information, to compensate the inferior image features encoded by CLIP. Through binding object and quantity information to minimizing the in-between interlacing between multiple objects, the FeCom module enhances the distinction and separability of each object attribute, thereby extracting object attributes and supporting high-quality editing.

Object Preservation. The FeCom module consists of three key components, as illustrated in Fig. 2, a CLIP-based image encoder $CLIP(\cdot)$, a feature attention mechanism, and a feature compensation mechanism. First, the input image I is encoded into $CLIP(I)$, while the text prompt c_q serves as input to the attention mechanism. The feature attention mechanism maps object-specific quantity information from the text prompt onto $CLIP(I)$, identifying gaps in the encoded image features. This process generates compensation features that align with the original image features. Mathematically, this interaction is expressed as:

$$I_c = \text{Softmax}\left(\frac{Q_g K_t^T}{\sqrt{d_k}}\right) V_t, \quad (1)$$

$$K_t = F(c_q), V_t = F(c_q), Q_g = F(CLIP(I)),$$

with $F(\cdot)$ representing an MLP layer. The resulting compensation features I_c are then added to $CLIP(I)$ to produce enhanced image features I_g , ensuring the distinction and separability of each object attribute. This process is formulated as:

$$F(I, c_q) = I_g = CLIP(I) + \lambda I_c, \quad (2)$$

where λ is a tunable scaling factor.

The motivation for this approach, as illustrated in Fig. 3 (b), even when Gaussian noise $\mathcal{N}(0, 1)$ is added to the image features extracted by CLIP and used as I_g in the QTTN module, the resulting images do not degrade into incomprehensible or low-quality outputs. Instead, the added noise primarily alters object attributes, background, and style while preserving the structure and clarity of the image. This observation highlights that the source of aliasing of object attributes lies in limited ability of CLIP to minimize the in-between interlacing and encode attribute for each object.

Through this design, the FeCom module ensures the distinction and separability of each object attribute, enabling the model to extract object attributes during editing. Moreover, it enhances the handling of fine image details, ensuring that MoEdit consistently generates high-quality images.

3.3. Quantity Attention

This module performs two key tasks. First, it treats an image as a unified whole to extract global information, enabling consistent quantity perception essential for quantity preservation. Second, it defines the attribute boundary of each object from enhanced image features I_g , which is crucial for high editability. Notably, the module relies solely on internal feature interactions to address these tasks, eliminating the need for auxiliary tools. This approach significantly reduces training costs and enhances user convenience.

Quantity-Perception Control. The QTTN module consists of three components, as illustrated in Fig. 4, the extraction module E_t , attention interaction, and U-Net injection. First, the enhanced image features I_g refined by the FeCom

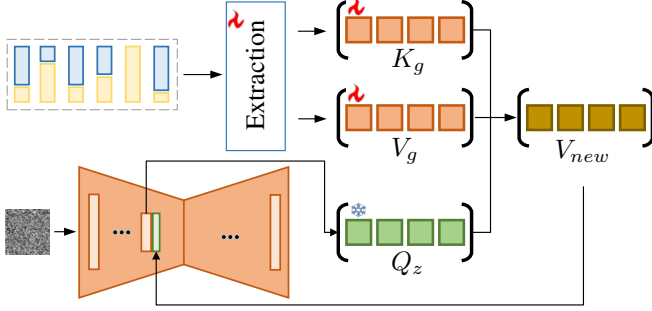


Figure 4. The framework of QTTN module. The Extraction module perceives the information of each object both individually and part of the whole image. Subsequently, an attention mechanism is employed to convert this information into a format compatible with the U-Net architecture, thereby ensuring that the consistent quantity perception provided by the QTTN module effectively controls the editing process.

module, and the input noise z_t^4 from the fourth block B_4 of the U-Net are obtained. Next, E_t extracts the information of each object both individually and part of the whole image from the mixed context I_g , which are then passed to the attention interaction stage to interact with z_t^4 . This process ensures that the format of quantity perception generated by QTTN module is compatible with the U-Net architecture. Mathematically, this is represented as:

$$\begin{aligned} \mathcal{Q}(I_g, z_t^4) = V_{new} &= \text{Softmax}\left(\frac{Q_z K_g^T}{\sqrt{d_k}}\right) V_g, \\ K_g = F(E_t(I_g)), V_g &= F(E_t(I_g)), Q_z = F(z_t^4), \end{aligned} \quad (3)$$

where $F(\cdot)$ denotes an MLP layer. The resulting V_{new} is directly injected into B_4 of the U-Net to control the editing process to ensure consistent quantity perception. The injection is defined as:

$$z_t^5 = \text{Attn}(Q_z, K_i, V_i) + \beta V_{new}, \quad (4)$$

where z_t^5 is the final output of B_4 and input to the fifth block B_5 of the U-Net. $\text{Attn}(Q_z, K_i, V_i)$ represents the cross-attention for text prompts c_e , β is a tunable scaling factor.

Insertion Point. Following prior studies [43], the U-Net is decomposed into 11 transformer blocks, denoted as B_i ($i = 1, 2, \dots, 11$). These blocks include four downsampling blocks, one middle block, and six upsampling blocks. The fourth block B_4 is chosen as the insertion point for the QTTN module, based on the functionality of each block [8]. As demonstrated in Sec. 4.4, the insertion point of the B_4 provides an optimal balance, allowing the U-Net to maximize the utility of consistent quantity perception while maintaining high editability.

This design empowers the QTTN module to enrich the U-Net model with consistent quantity perception, enabling effective control over object quantities and ensuring high editability during image editing.

3.4. Training and Inference

During the training phase, only MSE Loss was employed to guide the learning process. As shown in Fig. 2, user-provided text prompts for guiding image editing are replaced with null-text inputs. This prevents interference while retaining their utility for image editing. In the inference phase, users can input personalized text prompts to direct image editing toward their desired outputs.

4. Experiments

4.1. Implementation

The experiments are conducted using PyTorch on NVIDIA A6000 GPUs. This research utilized SDXL [32] as the baseline model and employed a CLIP model [33] pre-trained on the Laion-2B [35] as the image encoder. During training, all pre-trained weights remain frozen, while only the FeCom and QTTN module weights are fine-tuned. The scaling factors λ and β are both set to 1.0, with a learning rate of 0.00025. The Adam optimizer is used to perform optimization over 12,000 steps. Notably, MoEdit also supports single-image training and can perform editing on this image. Regarding the dataset, it comprises over 1,200 multi-object images (3 to 14 objects and 3 to 5 c_q per image). For evaluation, 30 test images are selected with 50 to 150 editing instructions per image, generating approximately 3,000 result images for quantitative evaluation. Selected results are analyzed in subsequent sections. The dataset will be expanded and made publicly available for future research.

4.2. Quantitative Comparisons

Seven algorithms are selected for comparison: SSR-Encoder [59], λ -Eclipse [31], IP-Adapter [57], Blip-diffusion [20], MS-diffusion [45], Emu2 [39], and TurboEdit [52], as summarized in Table 1. Six objective metrics are employed: HyperIQA [38], AesBench [11], Q-Align [50], NIQE [28], CLIP Score [9], and LPIPS [58]. These metrics evaluate various aspects: Perceptual Quality: NIQE, HyperIQA, and LPIPS focus on naturalness and visual fidelity. Semantic Consistency: CLIP Score quantifies alignment between generated images and text prompts. Visual Composition and Aesthetics: Q-Align and AesBench assess image composition and aesthetic quality. Additionally, two subjective metrics are adopted: Numerical Accuracy, measuring the percentage of successfully preserving quantity in the results, and MOS, reflecting the proportion of participants favoring a specific model. To collect subjective evaluations, 20 users are invited in image evaluation.

Method	Objective Metrics									Subjective Metrics							
	NIQE ↓	HyperIQA ↑	CLIP Score		LPIPS ↓	Q-Align		AesBench ↑	MOS ↑	Numerical ↑							
			Whole ↑	Edit ↑		Quality ↑	Aesthetic ↑			3	4	5	6	7	8	9	9+
SSR-Encoder [59]	3.106	62.16	0.2897	0.1897	0.2951	4.1175	3.7273	67.75	0.68	64.57	59.85	21.99	25.87	14.21	5.41	6.21	3.75
lambda-Eclipse [31]	3.552	65.42	0.2963	0.1821	0.3261	4.3247	4.1578	68.08	0.00	82.32	83.01	50.21	55.42	41.37	35.46	40.25	25.12
IP-Adapter [57]	2.952	71.19	0.2938	0.2218	0.3397	4.5724	4.2302	70.55	0.98	25.61	30.12	17.36	15.87	5.32	1.77	2.31	0.54
Blip-diffusion [20]	2.983	70.55	0.2913	0.2170	0.3797	4.3667	3.8476	65.16	0.00	52.26	30.18	10.77	4.93	3.27	5.01	0.77	0.91
MS-diffusion [45]	2.771	65.41	0.3043	0.2361	0.2904	4.7645	4.3633	74.45	7.68	74.33	51.26	38.21	21.36	24.32	27.05	13.2	5.68
Emu2 [39]	3.059	68.51	0.3012	0.2296	0.1875	4.7836	4.3528	75.09	3.87	92.82	93.04	88.76	82.56	84.57	80.75	82.97	73.46
TurboEdit [52]	2.872	71.72	0.3101	0.2427	0.1684	4.6849	4.2181	72.13	11.35	93.71	91.98	85.78	78.65	73.21	74.78	69.38	59.33
MoEdit(Ours)	2.749	75.66	0.3254	0.2557	0.2555	4.8763	4.6172	77.05	75.44	95.54	92.15	83.44	84.31	82.56	77.98	79.65	70.34

Table 2. Quantitative comparisons on six objective metrics and two subjective metrics. The best, second best and third best have been marked by red, blue and green respectively. MoEdit demonstrates superior performance across all objective metrics except LPIPS. In subjective evaluations, while Emu2 slightly outperformed MoEdit in Numerical Accuracy, MoEdit achieves a significant advantage in MOS. In particular, MoEdit produces high-quality edits that effectively preserve quantity consistency and extract object attributes, meeting user expectations and aesthetic preferences.



Figure 5. Qualitative comparisons. Blip-diffusion [20] struggles with editability and stability, while IP-Adapter [57] improves clarity but lacks robustness in quantity preservation. MS-diffusion [45] handles few objects well but fails with larger numbers. Emu2 [39] ensures structural consistency but limits editability. TurboEdit [52] balances tasks yet falls short in quantity and style handling. Finally, MoEdit successfully achieves a well-balanced performance in quantity consistency, semantic accuracy, stylistic consistency, and aesthetic quality.

A comprehensive evaluation is provided in Table 2. While TurboEdit achieves the highest LPIPS score, indicating strong perceptual similarity to original images, MoEdit outperforms all methods on the remaining metrics. On aver-

age, MoEdit demonstrates a 3.83% improvement across all metrics, with the most significant gain observed in aesthetic performance under Q-Align (5.82%) and the smallest in NIQE (0.79%). In subjective evaluations, MoEdit slightly

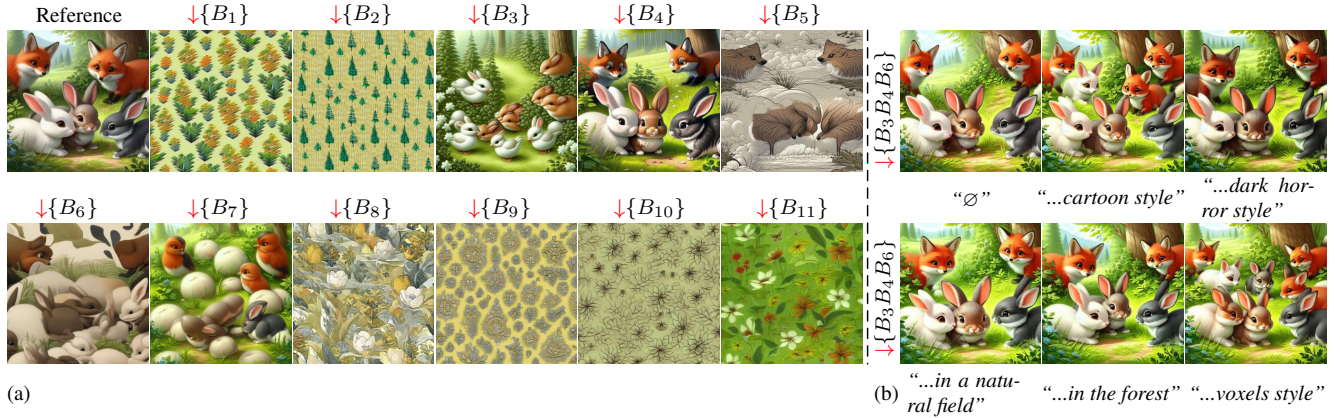


Figure 6. Effects of different insertion positions. Reference denotes the input image. $\downarrow B_i$ indicates the insertion of the Quantity Attention (QTTN) module into block B_i of the U-Net, while \emptyset signifies that the user text prompt is set to null-text. (a) The first and second rows show the results obtained by inserting the QTTN module into different blocks of the U-Net during training and applying null-text during inference. When the input image is inserted into B_4 , it effectively utilizes the quantity perception from the QTTN module. (b) The first and second rows demonstrate the image editing effects achieved by training with the QTTN module inserted into three blocks (B_3 , B_4 , B_6) simultaneously and applying varying user text prompts during inference.



Figure 7. Ablation study. The first row demonstrates that the exclusion of the Feature Compensation (FeCom) module results in significant instability in the visual representations of object attributes and image details. The second row demonstrates that the absence of the Quantity Attention (QTTN) module causes MoEdit to completely lose its capability of consistent quantity perception, leading to substantial disruptions in image structure and semantics. The final row showcases the full capability of MoEdit, which effectively completes editing tasks with high quality, preserving quantity consistency and extracting object attributes.

lags behind Emu2 in Numerical Accuracy due to the clustering strategy of Emu2, which enhances numerical stability in visualization but restricts editability. Overall, MoEdit ex-

cels in meeting user expectations and aesthetic preferences by extracting object attributes and ensuring consistent quantity perception during editing.

4.3. Qualitative Comparisons

Fig. 5 illustrates qualitative comparisons between MoEdit and seven competing methods on multi-object image editing tasks. Significant limitations are observed in SSR-Encoder, λ -Eclipse, and Blip-diffusion, including limited editability, instability in object attributes and quantity perception, image distortion, and inconsistency in structural and semantic alignment. While IP-Adapter shows slight advantages in clarity and realism due to its robust baseline model, it falls short of MoEdit. MS-diffusion demonstrates reasonable editability and quantity preservation when dealing with a small number of objects but struggles with larger numbers, often misinterpreting numerical constraints and object attributes. Emu2 maintains quantity and structural consistency well but frequently suffers from image distortion and over-clustering, limiting diversity and editability. TurboEdit achieves relatively balanced performance but trails MoEdit in critical aspects such as quantity preservation, editability, and handling complex style modifications. In contrast, MoEdit consistently delivers superior results, balancing semantic accuracy, stylistic consistency, and aesthetic quality. Its ability to extract object attributes and preserve quantity consistency while fulfilling user expectations sets it apart from other methods. For more qualitative demonstrations, please refer to Supplementary Material.

4.4. Ablation Study

Insertion point. Fig. 6 (a) illustrates the effectiveness of integrating quantity perception into U-Net when the QTTN module is inserted into a single block. Specifically,

QTTN	FeCom	NIQE ↓	HyperIQA ↑	CLIP Score	
				Whole ↑	Edit ↑
✗	✓	2.9988	71.82	0.2831	0.2687
✓	✗	2.6890	76.17	0.3052	0.2752
✓	✓	2.6501	77.87	0.3274	0.2790

QTTN	FeCom	LPIPS ↓	Numerical ↑	Q-Align	
				Quality ↑	Aesthetic ↑
✗	✓	0.3116	25.67	4.8945	4.4602
✓	✗	0.2777	82.31	4.9023	4.6562
✓	✓	0.2731	86.79	4.9219	4.8047

Table 3. Ablation study. Removing the FeCom module significantly reduces the whole metric in CLIP Score and aesthetics metric in Q-Align, due to the text-image mismatches and aliasing of object attributes, respectively, leading to failures in extracting object attributes. In contrast, removing the QTTN module causes declines across all metrics, including quantity preservation, structural consistency, editability, and aesthetics. These results demonstrate that the two modules are complementary to achieve the optimal performance of MoEdit.

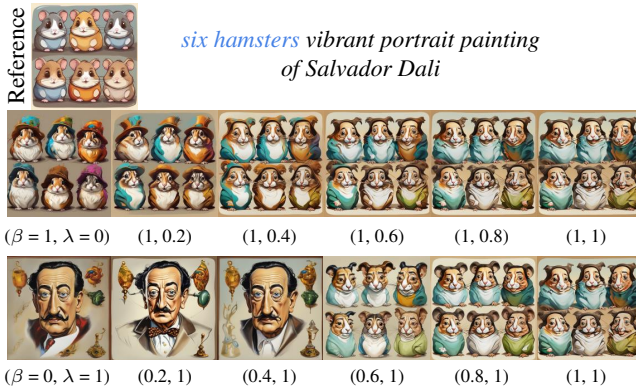


Figure 8. Scale variation. The first and second rows illustrate the variations in editing results when Reference and “vibrant portrait painting of Salvador Dali” are used as inputs, under different λ and β values. The numerical values below each image represent the corresponding λ and β settings. As λ decreases, the objects progressively lose the attributes of the “vibrant portrait painting of Salvador Dali”. Similarly, as beta decreases, MoEdit gradually loses its sensitivity to quantitative attributes.

when the QTTN module is incorporated into B_4 , U-Net effectively leverages quantity perception to enhance performance. In contrast, Fig. 6 (b) demonstrates the impact of injecting quantity perception into multiple blocks simultaneously. This approach disrupts the guidance provided by text prompts, significantly compromising editability and stability. Consequently, integrating the QTTN module exclusively into B_4 achieves an optimal trade-off between utilizing quantity perception and maintaining editability.

Module Effectiveness. Excluding the FeCom module (“w/o FeCom module”) from the pipeline leads to significant performance degradation, as shown in the first row of Fig. 7. The first and second columns reveal a severe

aliasing of object attributes, while the third column highlights the failure to extract the inherent juvenile characteristics of the entities in the input image. Together, these observations suggest an inability to effectively extract object attributes. Furthermore, the fourth column demonstrates a notable degradation of details in the output image. Similarly, removing the QTTN module (“w/o QTTN module”) produces results displayed in the second row of Fig. 7. The absence of the QTTN module impairs quantity perception, resulting in inconsistencies in object counts, image structures, and object semantics.

Table 3 quantifies these effects. Removing the FeCom module significantly reduces the whole and aesthetic metric in CLIP Score and Q-Align, respectively, primarily due to mismatches between object attributes and textual prompts, object attributes aliasing, and loss of image detail. In contrast, removing the QTTN results in notable declines across all metrics, including quantity perception, image quality, structural consistency, editability, and aesthetics. These findings highlight the complementary roles of the FeCom and QTTN in optimizing the performance of MoEdit.

Adjustable Scale Variation. Fig. 8 depicts how variations in λ and β during inference affect editing outcomes. Gradually reducing λ diminishes the “vibrant portrait painting of Salvador Dali” attribute in the six hamsters, which vanishes entirely when λ reaches 0. Similarly, decreasing β weakens the capability of quantity perception of QTTN module, leading to increased structural and semantic disorder in the generated images. When β is reduced to 0, the generated images lose structural and semantic coherence entirely.

5. Conclusion

This paper presents MoEdit, an novel auxiliary-free framework for multi-object image editing that addresses critical challenges in quantity perception and object attribute extraction. By integrating the FeCom and QTTN modules, MoEdit achieves SOTA performance in editing quality, object attributes extraction, and consistent quantity preservation. The FeCom module effectively reduces aliasing of object attributes, while the QTTN module ensures consistent quantity perception without reliance on auxiliary tools. Experimental results demonstrate the superiority of MoEdit over existing methods in terms of visual quality, semantic consistency, and editability. Future work can enhance the model robustness in complex interaction scenarios.

Acknowledgment

The work was supported in part by the National Natural Science Foundation of China under Grant 62301310 and 62176169, Sichuan Science and Technology Program under Grant 2024NSFSC1426, Science and Technology Development Fund of Macao Grant (0004/2024/E1B1) and Macao Polytechnic University Grant (RP/FCA-10/2023).

References

- [1] Omri Avrahami, Ohad Fried, and Dani Lischinski. Blended latent diffusion. *ACM transactions on graphics (TOG)*, 42(4):1–11, 2023. 2
- [2] Jacky Cao, Kit-Yung Lam, Lik-Hang Lee, Xiaoli Liu, Pan Hui, and Xiang Su. Mobile augmented reality: User interfaces, frameworks, and intelligence. *ACM Computing Surveys*, 55(9):1–36, 2023. 2
- [3] Goirik Chakrabarty, Aditya Chandrasekar, Ramya Hebbalaguppe, and AP Prathosh. Lomoe: Localized multi-object editing via multi-diffusion. In *ACM Multimedia 2024*, 2024. 2, 3
- [4] Ha-Yeong Choi, Sang-Hoon Lee, and Seong-Whan Lee. Dddm-vc: Decoupled denoising diffusion models with disentangled representation and prior mixup for verified robust voice conversion. In *Proceedings of the AAAI Conference on Artificial Intelligence*, pages 17862–17870, 2024. 2
- [5] Guillaume Couairon, Jakob Verbeek, Holger Schwenk, and Matthieu Cord. Diffedit: Diffusion-based semantic image editing with mask guidance. *arXiv preprint arXiv:2210.11427*, 2022. 2
- [6] Florinel-Alin Croitoru, Vlad Hondru, Radu Tudor Ionescu, and Mubarak Shah. Diffusion models in vision: A survey. *IEEE Transactions on Pattern Analysis and Machine Intelligence*, 45(9):10850–10869, 2023. 2
- [7] Xuehao Cui, Guangyang Wu, Zhenghao Gan, Guangtao Zhai, and Xiaohong Liu. Face2qr: A unified framework for aesthetic, face-preserving, and scannable qr code generation. *Advances in Neural Information Processing Systems*, 37:29142–29165, 2025. 2
- [8] Yarden Frenkel, Yael Vinker, Ariel Shamir, and Daniel Cohen-Or. Implicit style-content separation using b-lora. *arXiv preprint arXiv:2403.14572*, 2024. 5
- [9] Jack Hessel, Ari Holtzman, Maxwell Forbes, Ronan Le Bras, and Yejin Choi. Clipscore: A reference-free evaluation metric for image captioning. *arXiv preprint arXiv:2104.08718*, 2021. 5, 3, 4
- [10] Yuzhou Huang, Liangbin Xie, Xintao Wang, Ziyang Yuan, Xiaodong Cun, Yixiao Ge, Jiantao Zhou, Chao Dong, Rui Huang, Ruimao Zhang, et al. Smartedit: Exploring complex instruction-based image editing with multimodal large language models. In *Proceedings of the IEEE/CVF Conference on Computer Vision and Pattern Recognition*, pages 8362–8371, 2024. 3
- [11] Yipo Huang, Quan Yuan, Xiangfei Sheng, Zhichao Yang, Haoning Wu, Pengfei Chen, Yuzhe Yang, Leida Li, and Weisi Lin. Aesbench: An expert benchmark for multimodal large language models on image aesthetics perception. *arXiv preprint arXiv:2401.08276*, 2024. 5, 3, 4
- [12] Inbar Huberman-Spiegelglas, Vladimir Kulikov, and Tomer Michaeli. An edit friendly ddpm noise space: Inversion and manipulations. In *Proceedings of the IEEE/CVF Conference on Computer Vision and Pattern Recognition*, pages 12469–12478, 2024. 2
- [13] KJ Joseph, Prateeksha Udhayan, Tripti Shukla, Aishwarya Agarwal, Srikrishna Karanam, Koustava Goswami, and Balaji Vasan Srinivasan. Iterative multi-granular image editing using diffusion models. In *Proceedings of the IEEE/CVF Winter Conference on Applications of Computer Vision*, pages 8107–8116, 2024. 2
- [14] Bahjat Kawar, Shiran Zada, Oran Lang, Omer Tov, Huiwen Chang, Tali Dekel, Inbar Mosseri, and Michal Irani. Imagic: Text-based real image editing with diffusion models. In *Proceedings of the IEEE/CVF Conference on Computer Vision and Pattern Recognition*, pages 6007–6017, 2023. 2
- [15] Gwanhyeong Koo, Sunjae Yoon, and Chang D Yoo. Wavelet-guided acceleration of text inversion in diffusion-based image editing. In *ICASSP 2024-2024 IEEE International Conference on Acoustics, Speech and Signal Processing (ICASSP)*, pages 4380–4384. IEEE, 2024. 2
- [16] Jiyoung Lee, Joon Son Chung, and Soo-Whan Chung. Imaginary voice: Face-styled diffusion model for text-to-speech. In *ICASSP 2023-2023 IEEE International Conference on Acoustics, Speech and Signal Processing (ICASSP)*, pages 1–5. IEEE, 2023. 2
- [17] Chunyi Li, Zicheng Zhang, Haoning Wu, Wei Sun, Xiongkuo Min, Xiaohong Liu, Guangtao Zhai, and Weisi Lin. Agiqa-3k: An open database for ai-generated image quality assessment. *IEEE Transactions on Circuits and Systems for Video Technology*, 34(8):6833–6846, 2023. 2
- [18] Chunyi Li, Haoning Wu, Hongkun Hao, Zicheng Zhang, Tengchuan Kou, Chaofeng Chen, Xiaohong Liu, LEI BAI, Weisi Lin, and Guangtao Zhai. G-refine: A general refiner for text-to-image generation. In *ACM Multimedia 2024*, 2024. 2
- [19] Chunyi Li, Haoning Wu, Zicheng Zhang, Hongkun Hao, Kaiwei Zhang, Lei Bai, Xiaohong Liu, Xiongkuo Min, Weisi Lin, and Guangtao Zhai. Q-refine: A perceptual quality refiner for ai-generated image. In *2024 IEEE International Conference on Multimedia and Expo (ICME)*, pages 1–6. IEEE, 2024. 2
- [20] Dongxu Li, Junnan Li, and Steven Hoi. Blip-diffusion: Pre-trained subject representation for controllable text-to-image generation and editing. *Advances in Neural Information Processing Systems*, 36, 2024. 3, 5, 6, 4
- [21] Shiyu Li, Hannah Schieber, Niklas Corell, Bernhard Egger, Julian Kreimeier, and Daniel Roth. Gbot: graph-based 3d object tracking for augmented reality-assisted assembly guidance. In *2024 IEEE Conference Virtual Reality and 3D User Interfaces (VR)*, pages 513–523. IEEE, 2024. 2
- [22] Yanyu Li, Huan Wang, Qing Jin, Ju Hu, Pavlo Chemerys, Yun Fu, Yanzhi Wang, Sergey Tulyakov, and Jian Ren. Snapfusion: Text-to-image diffusion model on mobile devices within two seconds. *Advances in Neural Information Processing Systems*, 36, 2024. 2
- [23] Pengyang Ling, Lin Chen, Pan Zhang, Huaian Chen, Yi Jin, and Jinjin Zheng. Freedrag: Feature dragging for reliable point-based image editing. In *Proceedings of the IEEE/CVF Conference on Computer Vision and Pattern Recognition*, pages 6860–6870, 2024. 2
- [24] Haipeng Liu, Yang Wang, Biao Qian, Meng Wang, and Yong Rui. Structure matters: Tackling the semantic discrepancy in diffusion models for image inpainting. In *Proceedings of the IEEE/CVF Conference on Computer Vision and Pattern Recognition*, pages 8038–8047, 2024. 2

- [25] Jie Liu, Gongye Liu, Jiajun Liang, Ziyang Yuan, Xiaokun Liu, Mingwu Zheng, Xiele Wu, Qiulin Wang, Wenyu Qin, Menghan Xia, et al. Improving video generation with human feedback. *arXiv preprint arXiv:2501.13918*, 2025. 2
- [26] Alejandro Martin-Gomez, Haowei Li, Tianyu Song, Sheng Yang, Guangzhi Wang, Hui Ding, Nassir Navab, Zhe Zhao, and Mehran Armand. Sttar: surgical tool tracking using off-the-shelf augmented reality head-mounted displays. *IEEE Transactions on Visualization and Computer Graphics*, 2023. 2
- [27] Haruka Matsuda, Ren Togo, Keisuke Maeda, Takahiro Ogawa, and Miki Haseyama. Multi-object editing in personalized text-to-image diffusion model via segmentation guidance. In *ICASSP 2024-2024 IEEE International Conference on Acoustics, Speech and Signal Processing (ICASSP)*, pages 8140–8144. IEEE, 2024. 2
- [28] Anish Mittal, Rajiv Soundararajan, and Alan C Bovik. Making a “completely blind” image quality analyzer. *IEEE Signal processing letters*, 20(3):209–212, 2012. 5, 3, 4
- [29] Ron Mokady, Amir Hertz, Kfir Aberman, Yael Pritch, and Daniel Cohen-Or. Null-text inversion for editing real images using guided diffusion models. In *Proceedings of the IEEE/CVF Conference on Computer Vision and Pattern Recognition*, pages 6038–6047, 2023. 2
- [30] Chong Mou, Xintao Wang, Jiechong Song, Ying Shan, and Jian Zhang. Diffeditor: Boosting accuracy and flexibility on diffusion-based image editing. In *Proceedings of the IEEE/CVF Conference on Computer Vision and Pattern Recognition*, pages 8488–8497, 2024. 2
- [31] Maitreya Patel, Sangmin Jung, Chitta Baral, and Yezhou Yang. λ -eclipse: Multi-concept personalized text-to-image diffusion models by leveraging clip latent space. *arXiv preprint arXiv:2402.05195*, 2024. 3, 5, 6, 4
- [32] Dustin Podell, Zion English, Kyle Lacey, Andreas Blattmann, Tim Dockhorn, Jonas Müller, Joe Penna, and Robin Rombach. Sdxl: Improving latent diffusion models for high-resolution image synthesis. *arXiv preprint arXiv:2307.01952*, 2023. 2, 5, 1, 4
- [33] Alec Radford, Jong Wook Kim, Chris Hallacy, A. Ramesh, Gabriel Goh, Sandhini Agarwal, Girish Sastry, Amanda Askell, Pamela Mishkin, Jack Clark, Gretchen Krueger, and Ilya Sutskever. Learning transferable visual models from natural language supervision. In *ICML*, 2021. 5
- [34] Alec Radford, Jong Wook Kim, Chris Hallacy, Aditya Ramesh, Gabriel Goh, Sandhini Agarwal, Girish Sastry, Amanda Askell, Pamela Mishkin, Jack Clark, et al. Learning transferable visual models from natural language supervision. In *International conference on machine learning*, pages 8748–8763. PMLR, 2021. 2, 1
- [35] Christoph Schuhmann, Romain Beaumont, Richard Vencu, Cade Gordon, Ross Wightman, Mehdi Cherti, Theo Coombes, Aarush Katta, Clayton Mullis, Mitchell Wortsman, et al. Laion-5b: An open large-scale dataset for training next generation image-text models. *Advances in Neural Information Processing Systems*, 35:25278–25294, 2022. 5
- [36] Shelly Sheynin, Adam Polyak, Uriel Singer, Yuval Kirstain, Amit Zohar, Oron Ashual, Devi Parikh, and Yaniv Taigman. Emu edit: Precise image editing via recognition and generation tasks. In *Proceedings of the IEEE/CVF Conference on Computer Vision and Pattern Recognition*, pages 8871–8879, 2024. 2
- [37] Yujun Shi, Chuhui Xue, Jun Hao Liew, Jiachun Pan, Hanshu Yan, Wenqing Zhang, Vincent YF Tan, and Song Bai. Dragdiffusion: Harnessing diffusion models for interactive point-based image editing. In *Proceedings of the IEEE/CVF Conference on Computer Vision and Pattern Recognition*, pages 8839–8849, 2024. 2
- [38] Shaolin Su, Qingsen Yan, Yu Zhu, Cheng Zhang, Xin Ge, Jinqiu Sun, and Yanning Zhang. Blindly assess image quality in the wild guided by a self-adaptive hyper network. In *Proceedings of the IEEE/CVF conference on computer vision and pattern recognition*, pages 3667–3676, 2020. 5, 3, 4
- [39] Quan Sun, Yufeng Cui, Xiaosong Zhang, Fan Zhang, Qiyang Yu, Yueze Wang, Yongming Rao, Jingjing Liu, Tiejun Huang, and Xinlong Wang. Generative multimodal models are in-context learners. In *Proceedings of the IEEE/CVF Conference on Computer Vision and Pattern Recognition*, pages 14398–14409, 2024. 3, 5, 6, 4
- [40] Vadim Titov, Madina Khalmatova, Alexandra Ivanova, Dmitry Vetrov, and Aibek Alanov. Guide-and-rescale: Self-guidance mechanism for effective tuning-free real image editing. *arXiv preprint arXiv:2409.01322*, 2024. 2
- [41] Narek Tumanyan, Michal Geyer, Shai Bagon, and Tali Dekel. Plug-and-play diffusion features for text-driven image-to-image translation. In *Proceedings of the IEEE/CVF Conference on Computer Vision and Pattern Recognition*, pages 1921–1930, 2023. 2
- [42] Bram Wallace, Akash Gokul, and Nikhil Naik. Edict: Exact diffusion inversion via coupled transformations. In *Proceedings of the IEEE/CVF Conference on Computer Vision and Pattern Recognition*, pages 22532–22541, 2023. 2
- [43] Haofan Wang, Qixun Wang, Xu Bai, Zekui Qin, and Anthony Chen. Instantstyle: Free lunch towards style-preserving in text-to-image generation. *arXiv preprint arXiv:2404.02733*, 2024. 5
- [44] Xudong Wang, Trevor Darrell, Sai Saketh Rambhatla, Rohit Girdhar, and Ishan Misra. Instancediffusion: Instance-level control for image generation. In *Proceedings of the IEEE/CVF Conference on Computer Vision and Pattern Recognition*, pages 6232–6242, 2024. 2
- [45] X Wang, Siming Fu, Qihan Huang, Wangui He, and Hao Jiang. Ms-diffusion: Multi-subject zero-shot image personalization with layout guidance. *arXiv preprint arXiv:2406.07209*, 2024. 3, 5, 6, 4
- [46] Yibin Wang, Weizhong Zhang, Jianwei Zheng, and Cheng Jin. Enhancing object coherence in layout-to-image synthesis. *arXiv preprint arXiv:2311.10522*, 2023. 2
- [47] Zhenyu Wang, Aoxue Li, Zhenguo Li, and Xihui Liu. Genartist: Multimodal llm as an agent for unified image generation and editing. *arXiv preprint arXiv:2407.05600*, 2024. 3
- [48] Zhen Wang, Dongyuan Li, and Renhe Jiang. Diffusion models in 3d vision: A survey. *arXiv preprint arXiv:2410.04738*, 2024. 2

- [49] Guangyang Wu, Xiaohong Liu, Jun Jia, Xuehao Cui, and Guangtao Zhai. Text2qr: Harmonizing aesthetic customization and scanning robustness for text-guided qr code generation. In *Proceedings of the IEEE/CVF Conference on Computer Vision and Pattern Recognition*, pages 8456–8465, 2024. 2
- [50] Haoning Wu, Zicheng Zhang, Weixia Zhang, Chaofeng Chen, Liang Liao, Chunyi Li, Yixuan Gao, Annan Wang, Erli Zhang, Wenxiu Sun, et al. Q-align: Teaching llms for visual scoring via discrete text-defined levels. *arXiv preprint arXiv:2312.17090*, 2023. 5, 3, 4
- [51] Tsung-Han Wu, Long Lian, Joseph E Gonzalez, Boyi Li, and Trevor Darrell. Self-correcting llm-controlled diffusion models. In *Proceedings of the IEEE/CVF Conference on Computer Vision and Pattern Recognition*, pages 6327–6336, 2024. 2, 3
- [52] Zhengyi Wu, Nathaniel I. Kolkin, Jonathan Brandt, Richard Zhang, and Eli Shechtman. Turboedit: Real-time text-based disentangled real image editing. In *Proceedings of the European Conference on Computer Vision (ECCV)*, 2024. 1, 2, 3, 5, 6, 4
- [53] Sihan Xu, Yidong Huang, Jiayi Pan, Ziqiao Ma, and Joyce Chai. Inversion-free image editing with natural language. *arXiv preprint arXiv:2312.04965*, 2023. 2
- [54] Sihan Xu, Yidong Huang, Jiayi Pan, Ziqiao Ma, and Joyce Chai. Inversion-free image editing with language-guided diffusion models. In *Proceedings of the IEEE/CVF Conference on Computer Vision and Pattern Recognition*, pages 9452–9461, 2024. 2
- [55] Liumeng Xue, Chaoren Wang, Mingxuan Wang, Xueyao Zhang, Jun Han, and Zhizheng Wu. Singvisio: Visual analytics of diffusion model for singing voice conversion. *arXiv preprint arXiv:2402.12660*, 2024. 2
- [56] Yiwei Yang, Zheyuan Liu, Jun Jia, Zhongpai Gao, Yunhao Li, Wei Sun, Xiaohong Liu, and Guangtao Zhai. Diffstega: towards universal training-free coverless image steganography with diffusion models. *arXiv preprint arXiv:2407.10459*, 2024. 2
- [57] Hu Ye, Jun Zhang, Sibao Liu, Xiao Han, and Wei Yang. Ip-adapt: Text compatible image prompt adapter for text-to-image diffusion models. *arXiv preprint arXiv:2308.06721*, 2023. 3, 5, 6, 4
- [58] Richard Zhang, Phillip Isola, Alexei A Efros, Eli Shechtman, and Oliver Wang. The unreasonable effectiveness of deep features as a perceptual metric. In *Proceedings of the IEEE conference on computer vision and pattern recognition*, pages 586–595, 2018. 5, 3, 4
- [59] Yuxuan Zhang, Yiren Song, Jiaming Liu, Rui Wang, Jinpeng Yu, Hao Tang, Huaxia Li, Xu Tang, Yao Hu, Han Pan, et al. Ssr-encoder: Encoding selective subject representation for subject-driven generation. In *Proceedings of the IEEE/CVF Conference on Computer Vision and Pattern Recognition*, pages 8069–8078, 2024. 3, 5, 6, 4
- [60] Zhixing Zhang, Ligong Han, Arnab Ghosh, Dimitris N Metaxas, and Jian Ren. Sine: Single image editing with text-to-image diffusion models. In *Proceedings of the IEEE/CVF Conference on Computer Vision and Pattern Recognition*, pages 6027–6037, 2023. 2
- [61] Zicheng Zhang, Chunyi Li, Wei Sun, Xiaohong Liu, Xiongkuo Min, and Guangtao Zhai. A perceptual quality assessment exploration for aigc images. In *2023 IEEE International Conference on Multimedia and Expo Workshops (ICMEW)*, pages 440–445. IEEE, 2023. 2
- [62] Zhiyuan Zhang, DongDong Chen, and Jing Liao. Sgedit: Bridging llm with text2image generative model for scene graph-based image editing. *arXiv preprint arXiv:2410.11815*, 2024. 3
- [63] Zicheng Zhang, Haoning Wu, Chunyi Li, Yingjie Zhou, Wei Sun, Xiongkuo Min, Zijian Chen, Xiaohong Liu, Weisi Lin, and Guangtao Zhai. A-bench: Are llms masters at evaluating ai-generated images? *arXiv preprint arXiv:2406.03070*, 2024. 2
- [64] Shihao Zhao, Dongdong Chen, Yen-Chun Chen, Jianmin Bao, Shaozhe Hao, Lu Yuan, and Kwan-Yee K Wong. Uni-controlnet: All-in-one control to text-to-image diffusion models. *Advances in Neural Information Processing Systems*, 36, 2024. 2

MoEdit: On Learning Quantity Perception for Multi-object Image Editing

Supplementary Material

A. Details of Network Architecture

This section provides a detailed explanation of the design of two key modules in MoEdit: the Feature Compensation (FeCom) module and the Quantity Attention (QTTN) module. It covers their structural composition, dimensional transformations, inputs, and outputs. The FeCom module is designed to minimize interlacing during the extraction of object attributes, while the QTTN module ensures consistent quantity preservation.

A.1. Feature Compensation Module

A.1.1 Overall

This module processes an input image I and a text prompt c_q , which specifies objects and their quantities, to generate an enhanced feature I_g , characterized by distinct and separable object attributes. The module is composed of three main components: an image encoder (from CLIP [34]), a text encoder (from SDXL [32]), and a feature attention mechanism. The feature attention mechanism aligns textual and visual representations of object and quantity information, enabling effective extraction of object attributes. Fig. 9 provides a detailed overview of the FeCom module, with each step annotated to indicate its function. The notation “ $\rightarrow (...)$ ” represents the output dimensions at each stage.

A.1.2 Discussion of LayerNorm

The FeCom module incorporates a LayerNorm layer, which is critical for balancing original image features, aligning textual and visual information, and enabling the QTTN module to effectively consider each object both individually and part of the whole image. Fig. 10 underscores its significance, with Reference representing the input image.

In Fig. 10 (a), “m/o LayerNorm” denotes the results obtained when the LayerNorm layer from Fig. 9 is repositioned to the final stage, after the last fully connected (FC) layer, during training. This adjustment leads to a marked decline in both quantity consistent perception and object attributes extraction. Conversely, “w/o LayerNorm” refers to the scenario where the LayerNorm layer is entirely removed during training. While this configuration preserves quantity consistency, it introduces aliasing of object attributes.

In Fig. 10 (b), to elucidate these degradations, we analyze the original image features extracted by the image encoder of CLIP and the compensation features generated by the FeCom module. “Compensation Features (m/o)” refers to compensation features obtained under the “m/o LayerNorm” condition, with a value range of $[3, -3]$, while the

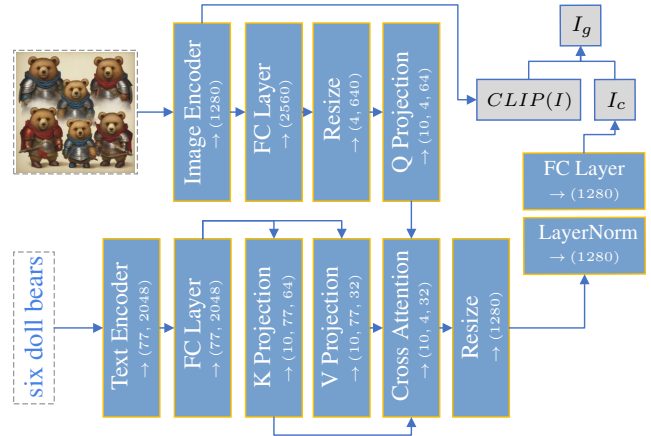


Figure 9. The detailed structure diagram of FeCom module. The image encoder is derived from CLIP [34], and the text encoder is sourced from SDXL [32]. The module takes two inputs—images and text prompts—and generates a single output: enhanced features I_g . In this process, $CLIP(I)$ denotes the inferior image features extracted by the image encoder of CLIP, while I_c represents the compensation features used to enhance it. Each step is explicitly defined, with “ $\rightarrow (...)$ ” denoting the dimensionality of the corresponding output.

original image features span $[4, -6]$. This narrow range suggests insufficient feature intensity, which fails to adequately mitigate the in-between interlacing in inferior original image features, thereby compromising quantity consistent perception and object attributes extraction. Conversely, “Compensation Features (w/o)” are produced under the “w/o LayerNorm” condition, with a value range of $[60, -80]$. This excessively broad range indicates over-suppression of original image features, resulting in substantial information loss, particularly in object attributes. In comparison, the compensation features constructed by the FeCom module in MoEdit (denoted as “Compensation Features (Ours)”) fall within a balanced range of $[15, -10]$. This range effectively preserves the original image information while minimizing in-between interlacing.

The quantitative comparisons are shown in Table 4. Notably, the “m/o LayerNorm” have a significant impact on the overall performance of MoEdit, primarily due to their limited compensatory capacity. In contrast, under the “w/o LayerNorm” condition, despite the excessive strength of the compensation features, image aesthetics, quality, and numerical accuracy remain largely unaffected. This stability can be attributed to the fact that these compensation fea-

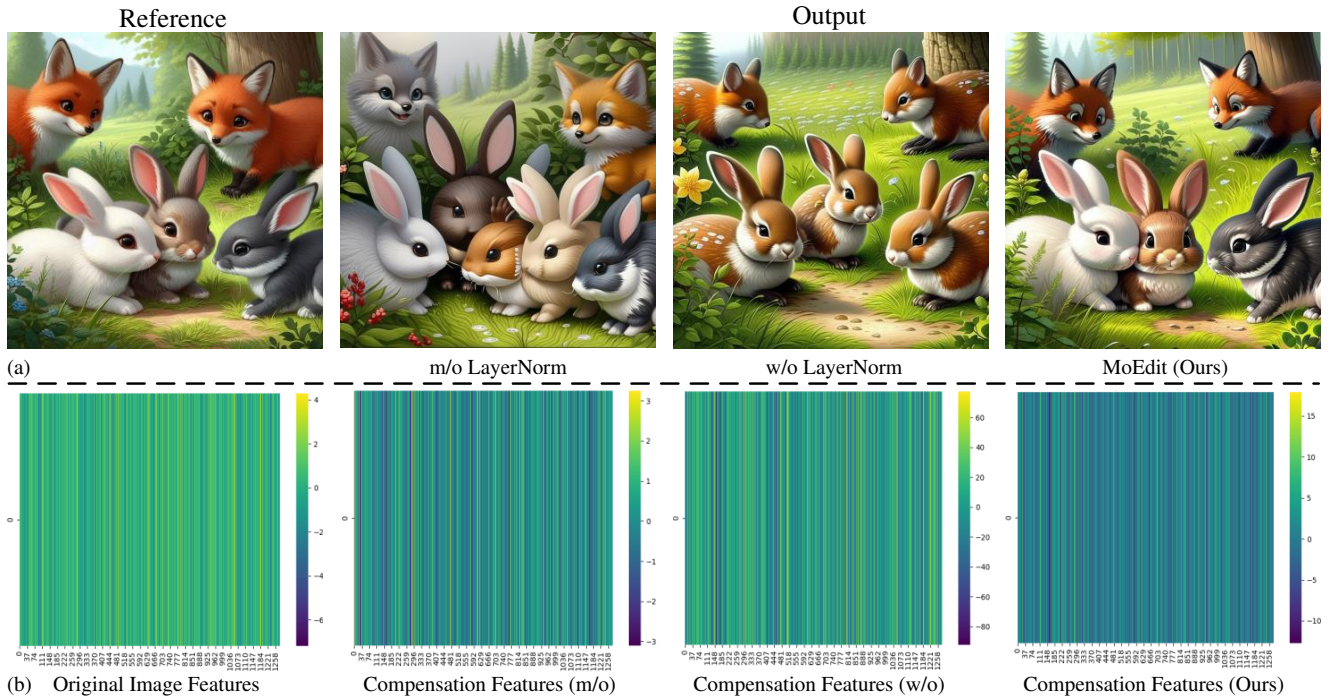


Figure 10. The importance of the LayerNorm layer. Please refer to Sec. A.1.2 for a comprehensive evaluation and detailed discussions regarding these configurations.

tures are derived from textual prompts containing object and quantity information. However, the loss of object attributes leads to a noticeable decline in textual-visual alignment and the similarity between the original and resulting images.

As demonstrated in Fig. 10 (a), MoEdit achieves superior performance visually in both preserving quantity consistency and extracting object attributes.

A.2. Quantity Attention Module

A.2.1 Overall

The module takes as input the image features I_g , enhanced by the FeCom module, and the noise z_t^4 from the fourth block B_4 of the U-Net. It outputs perception information of quantity consistency that can be interpreted by the U-Net to regulate the entire editing process. The module comprises three key components: the extraction module E_t , attention interaction, and U-Net injection. E_t is designed to disentangle each object attribute from the whole I_g while simultaneously capturing the global information of I_g . The attention interaction component translates the information extracted by E_t into a format that is interpretable by the U-Net. Finally, the U-Net injection component leverages this transformed information to control the image editing process, preserving quantity consistency. Fig. 11 presents the detailed structure of the QTTN module, with each step annotated to indicate its function. The notation “ \rightarrow (...)” represents the output dimensions at each stage.

Method	NIQE ↓	HyperIQA ↑	CLIP Score	
			Whole ↑	Edit ↑
m/o LayerNorm	2.8726	73.28	0.3005	0.2689
w/o LayerNorm	2.7081	75.99	0.3078	0.2778
w/o Extraction	2.7232	75.47	0.3105	0.2782
MoEdit (Ours)	2.6501	77.87	0.3274	0.2790

Method	LPIPS ↓	Numerical ↑	Q-Align	
			Quality ↑	Aesthetic ↑
m/o LayerNorm	0.3101	32.65	4.7511	4.4371
w/o LayerNorm	0.2943	84.77	4.8933	4.7552
w/o Extraction	0.2975	78.73	4.8344	4.6211
MoEdit (Ours)	0.2731	86.79	4.9219	4.8047

Table 4. Quantitative comparisons. “m/o LayerNorm” denotes the results obtained when the LayerNorm layer from Fig. 9 is repositioned to the final stage, after the last FC layer, during training. “w/o LayerNorm” refers to the scenario where the LayerNorm layer is entirely removed during training. “w/o Extraction” illustrates the absence of Extraction module in Fig. 11. For more discussion, please refer to Secs. A.1.2 and A.2.2.

A.2.2 Discussion of Extraction

In the QTTN module, E_t is a critical component. Although implemented by a single FC layer, E_t extracts clear and structured information about each object both individually and part of the whole I_g . This functionality cannot be directly incorporated into the attention interaction process. Fig. 12 underscores the importance of E_t , with the “w/o

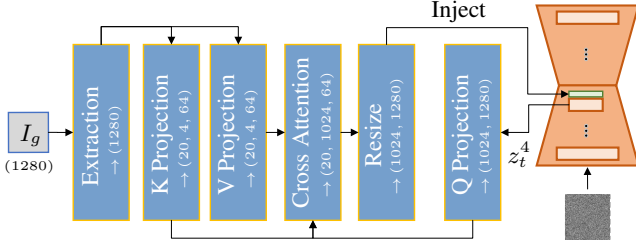


Figure 11. The detailed structure diagram of QTTN module. Each step is annotated with its specific purpose, with “ \rightarrow (...)” denoting the dimensionality of the corresponding output. This module receives two inputs: I_g , originating from the FeCom module, and input noise z_t^4 , from the fourth block B_4 of the U-Net. Its primary purpose is to generate a quantity consistent perception that can be effectively interpreted by the U-Net. The core of the Extraction module E_t is a FC layer, which is designed to consider each object both individually and part of the whole I_g . The functionality of E_t is detailed in Fig. 12.



Figure 12. The importance of the E_t . Please refer to Sec. A.2.2 for a comprehensive evaluation and detailed discussions regarding these configurations.

Extraction” condition illustrating its absence.

Without E_t , the distinctive and separable object attributes in I_g can still ensure quantity consistent perception. However, compared to MoEdit, the absence of E_t leads to suboptimal object attributes extraction, reduced image details, and poor anatomical representations. This limitation arises because the Q, K, and V Projections within the attention interaction cannot effectively handle both the extraction of each object information and the transformation of information patterns simultaneously. Therefore, MoEdit incorporates an independent FC layer to ensure the high quality information of each object required for effective attention interactions. This unique functionality underscores the rationale for designating this FC layer as Extraction.

The quantitative comparisons are summarized in Table 4. Notably, “w/o Extraction” exhibits a decline across multiple metrics, including image aesthetics, quality, text-image alignment, similarity between original and resulting images, and numerical accuracy.

B. Supplementary Experiments

B.1. Full Qualitative Comparisons

In our main paper, MoEdit was comprehensively evaluated using six objective metrics, HyperIQA [38], AesBench [11], Q-Align [50], NIQE [28], CLIP Score [9], and LPIPS [58], and two subjective metrics, MOS and Numerical Accuracy. The evaluation compared MoEdit against seven methods: SSR-Encoder [59], λ -Eclipse [31], IP-Adapter [57], Blip-diffusion [20], MS-diffusion [45], Emu2 [39], and TurboEdit [52]. This section provides additional details on these comparison methods and summarizes the code sources for all methods and evaluation metrics in Table 5, facilitating future research replication.

SSR-Encoder. This method is tailored for subject-driven generative tasks, encoding selective subject representations. By focusing on extracting and representing subject-specific features, it enhances the ability to maintain subject consistency in generated outputs.

λ -Eclipse. A multi-concept text-to-image generation model that leverages the latent space of CLIP to achieve efficient multimodal alignment. This method allows the flexible integration of multiple concepts while preserving semantic consistency between textual and visual inputs.

IP-Adapter. A text-compatible image-prompt adapter designed for text-to-image diffusion models. The introduction of efficient adapter modules enables the model to utilize image prompts to enhance generation quality while maintaining compatibility with textual input.

Blip-diffusion. This method combines pre-trained subject representations with text-to-image generation and editing. By integrating precise subject modeling, it offers more controllable image generation and editing while improving semantic alignment between text and images.

MS-diffusion. A method for multi-subject image personalization that integrates layout guidance for structured scene control. This method generates multi-subject, layout-accurate images in zero-shot scenarios, enhancing the diversity and consistency of outputs.

Emu2. This study investigates the contextual learning capabilities of generative multimodal models, showcasing their ability to perform diverse tasks in unsupervised settings via input prompts. The findings highlight the potential of these models for cross-task generalization and implicit learning, underscoring their flexibility and adaptability.

TurboEdit. An efficient text-driven image editing method that rapidly generates modifications aligned with textual descriptions. By optimizing the editing workflow, it provides a real-time, interactive image editing experience.

Due to space constraints in the main paper, qualitative comparisons were limited to conditions 3, 7, and 9+. In this section, results for the remaining conditions are presented in Figs. 13–17. Furthermore, Fig. 18 offers additional visual

Method	URL
SSR-Encoder	[59] https://github.com/Xiaojiu-z/SSR_Encoder
λ -Eclipse	[31] https://github.com/eclipse-t2i/lambda-eclipse-inference
IP-Adapter	[57] https://github.com/tencent-ailab/IP-Adapter
Blip-diffusion	[20] https://github.com/salesforce/LAVIS/tree/main/projects/blip-diffusion
MS-diffusion	[45] https://github.com/MS-Diffusion/MS-Diffusion
Emu2	[39] https://github.com/baaivision/Emu
TurboEdit	[52] https://betterze.github.io/TurboEdit/
Metric	URL
HyperIQA	[38] https://github.com/SSL92/hyperIQA
Q-Align	[50] https://github.com/Q-Future/Q-Align
AesBench	[11] https://github.com/yipoh/AesBench
NIQE	[28] https://github.com/csjunxu/Bovik_NIQE_SPL2013
CLIP Score	[9] https://github.com/Taited/clip-score
LPIPS	[58] https://github.com/richzhang/PerceptualSimilarity

Table 5. Code sources of seven comparison methods and six objective metrics

demonstrations of MoEdit output.

B.2. Visualization of Ablation Results

Scale variation. Due to the limited space in the main paper, we presented only the results for $\lambda = 1$ with varying β and $\beta = 1$ with varying λ . However, these results alone are insufficient to fully capture the mechanisms of the two modules. To address this, more comprehensive results are provided in Fig. 19, offering a clearer demonstration of the interaction between the modules.

When λ is fixed, increasing β enhances the ability of the QTTN module to disentangle each object attribute from the whole image and to extract global information, resulting in higher-quality outputs. This improvement, however, relies heavily on the input features I_g of the QTTN module, which must exhibit sufficient distinction and separability of object attributes. Conversely, when β is fixed, reducing λ increases the degree of aliasing of object attributes. Consequently, the QTTN module becomes less effective at extracting information of each object both individual and part of the whole, leading to a deterioration in the output quality.

B.3. Limitations

When the spatial relationship between objects and their surrounding 3D environment changes, MoEdit often struggles to deliver satisfactory editing results. This limitation stems from the baseline model, SDXL [32], which lacks the capability to effectively construct accurate 3D relationships in multi-object scenes. As illustrated in Fig. 20, prompts like “*on the table*” require consideration of not only the interaction between existing objects and their environment

but also the 3D spatial alignment between the newly introduced table and multiple objects. This challenge results in MoEdit producing artifacts such as misaligned object segments, truncation, and loss of surrounding elements like clothing. Meanwhile, other methods exhibit even poorer performance, either failing to achieve meaningful edits or simply modifying the ground to a wooden texture, thereby creating an illusion of objects being placed on a table. To address these challenges, future work could focus on integrating 3D environmental data, transcending the limitations of 2D information, to achieve better alignment and coherence between multi-object and their scenes.

Reference



four lego houses

IP-Adapter



Blip-diffusion



MS-diffusion



Emu2



TurboEdit



MoEdit (Ours)



"...futuristic metropolis style"

"...block print style"

"...made of crystal"

"→skyscrapers"

"→puppy houses"

Figure 13. Qualitative comparisons among a set of four objects.

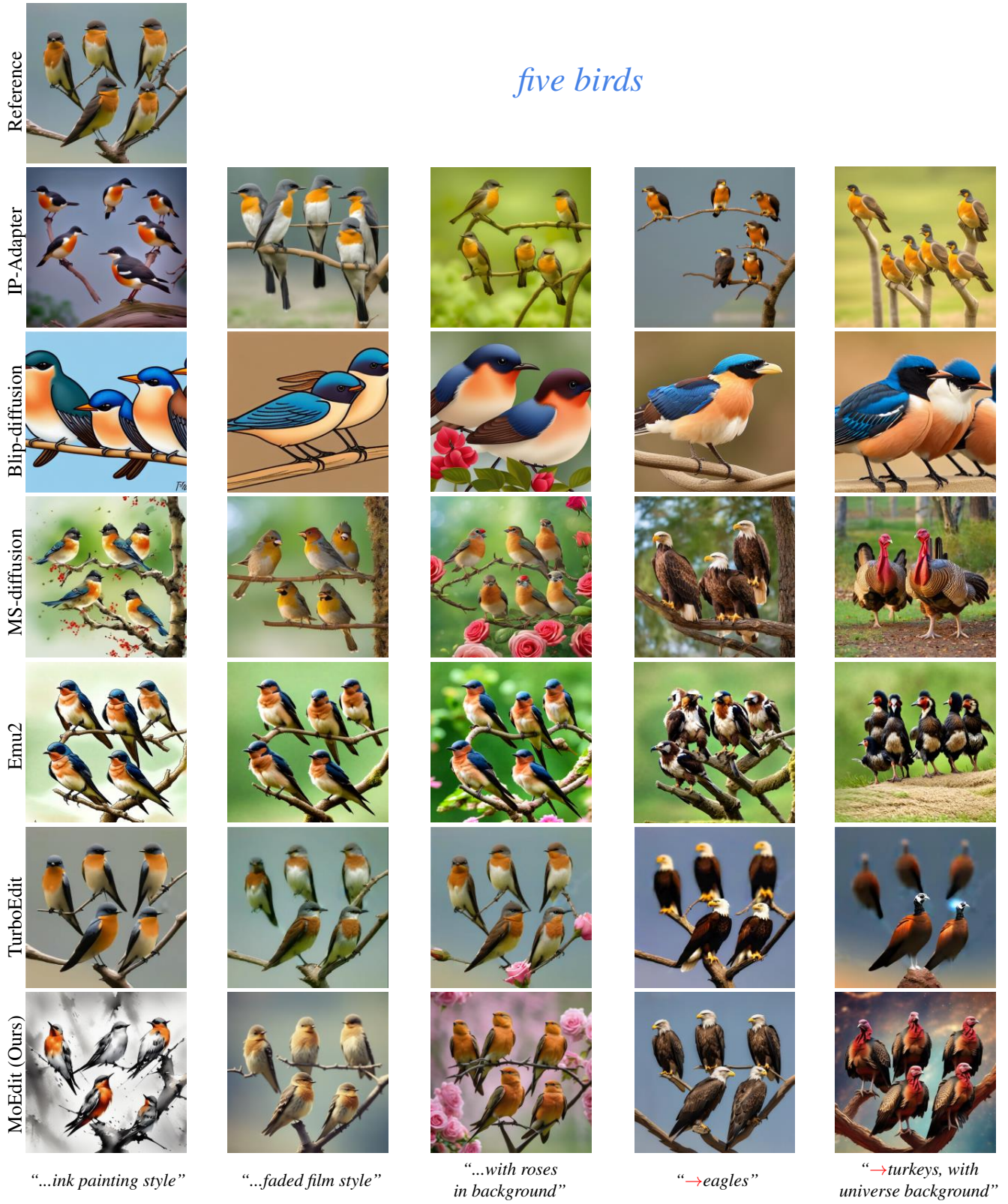


Figure 14. Qualitative comparisons among a set of five objects.

three lions, two pandas and a gorilla

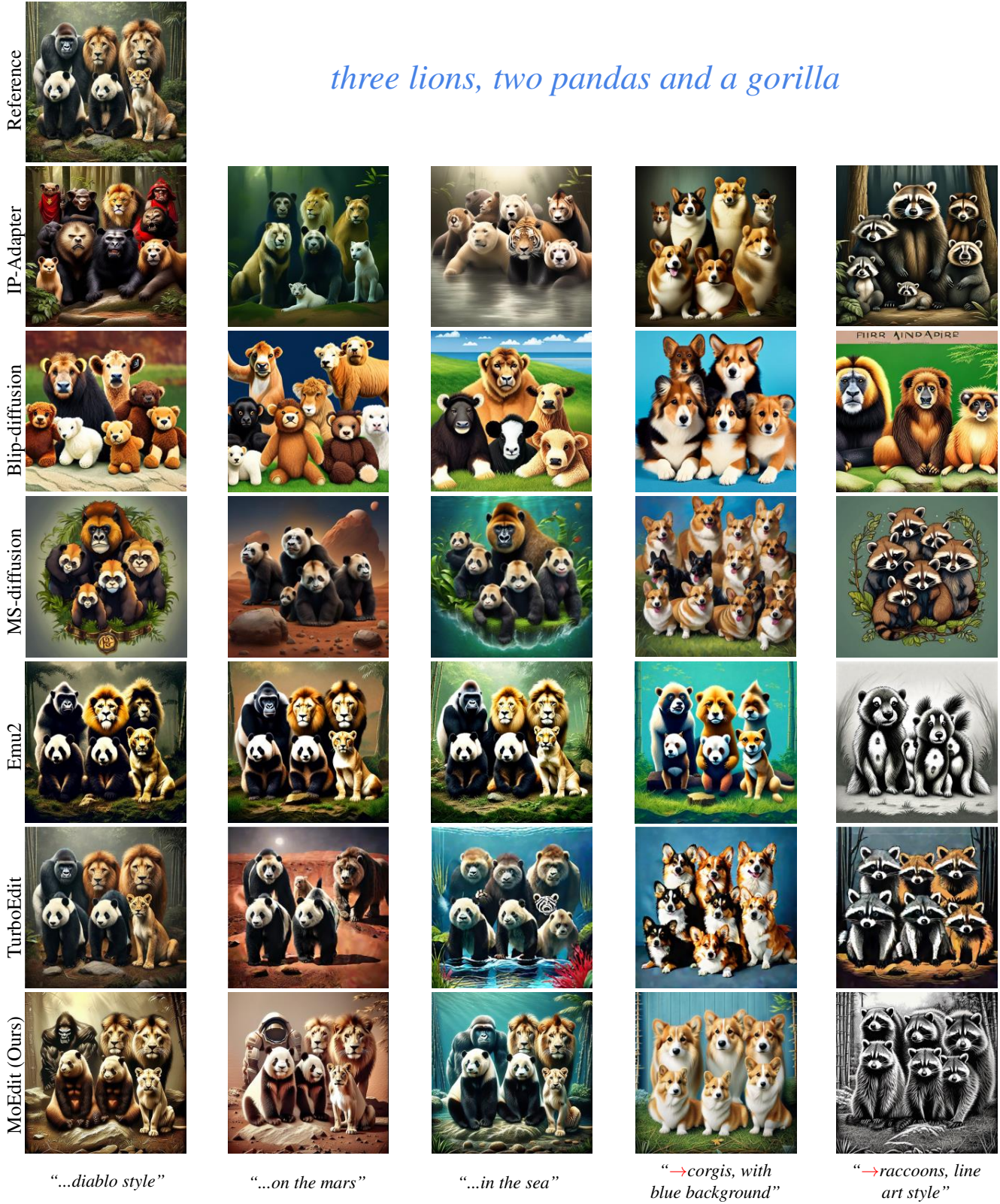


Figure 15. Qualitative comparisons among a set of six objects.

four people and four dogs



Figure 16. Qualitative comparisons among a set of eight objects.



Figure 17. Qualitative comparisons among a set of nine objects.

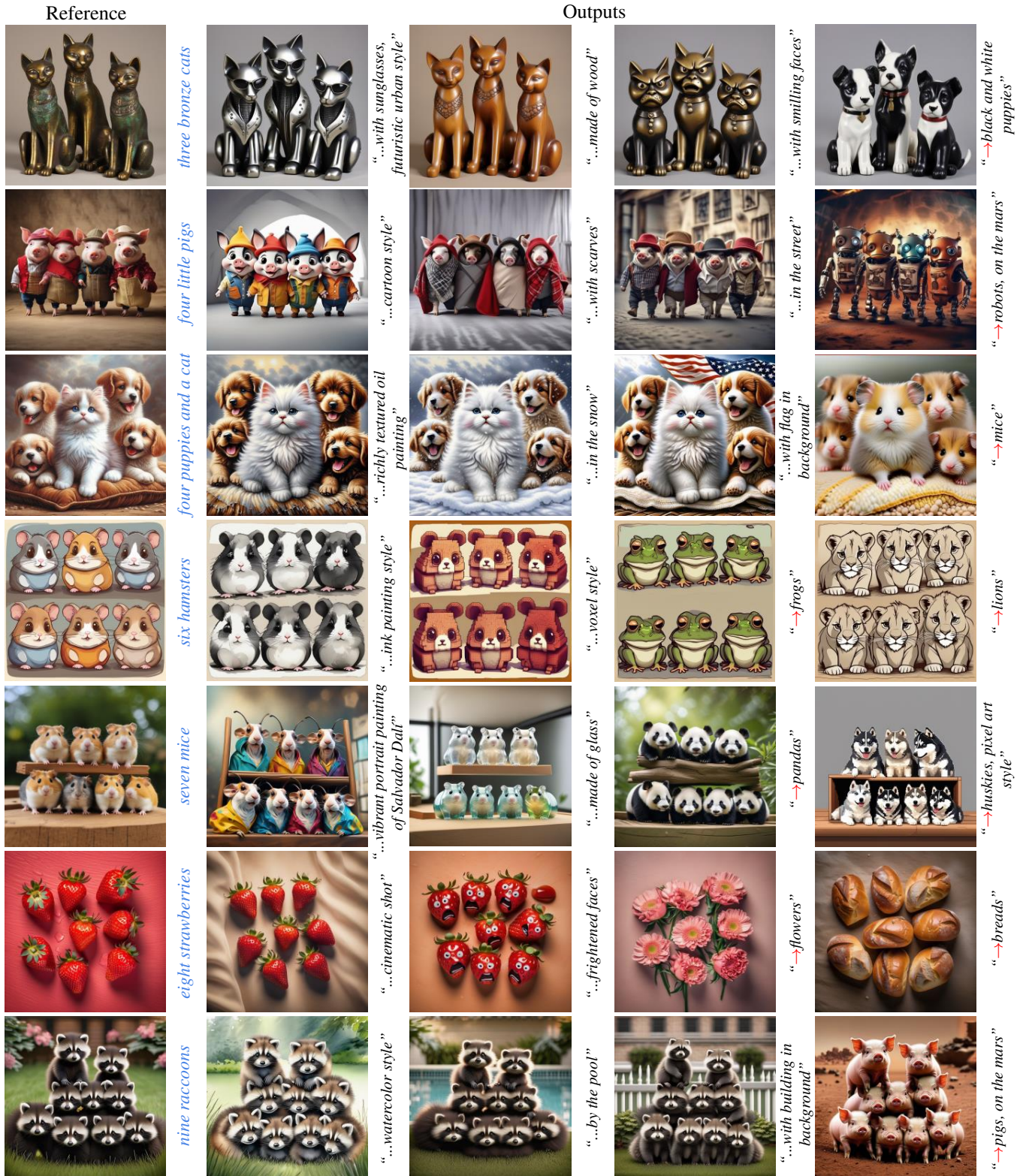


Figure 18. Additional qualitative results.



Figure 19. Scale variation. The reference image of all results are referred to Fig. 10. The top-left image illustrates the outcome when $(\lambda = 0, \beta = 0)$. Each row corresponds to results obtained with a fixed β and varying λ . From left to right, λ increases incrementally, as indicated by $\uparrow x$, where x denotes the increment from the baseline $\lambda = 0$. Similarly, each column corresponds to results generated with a fixed λ and varying β . From top to bottom, β increases incrementally, marked by $\uparrow x$, where x represents the increment from the baseline $\beta = 0$. Detailed discussions of these results are provided in Sec. B.2.



Figure 20. The illustration of limitations. The reference refers to the input image. All output images are edited based on the text prompts “on the table”. For more discussion, please refer to Sec. B.3.